The depth-inversion problem in shallow water [1]

Stéphan T. Grilli, Member ASCE [2]

Abstract : Two Depth Inversion Algorithms (DIAs) were developed and validated using on results of computations for the shoaling of periodic waves over mild slopes, in a two-dimensional numerical wave tank, based on fully nonlinear potential flow theory. The first algorithm, DIA1, uses sets of values of wave celerity c, height H, and spatial wavelengths L_c and L_t, simultaneously measured at a number of locations x_i ($i = 1, ..., N$) in the direction of wave propagation (e.g., using remote sensing techniques), to predict the depth variation $h(x_i)$. The second algorithm, DIA2, uses spatial wave asymmetry s_2/s_1 calculated from wave phase, instead of H. Results indicate that state-of-the-art depth inversion methods based on the linear dispersion relation may lead to large errors (50-70%) for the depth prediction in very shallow water, whereas the present methods are 3-10 times more accurate.

Introduction

A detailed knowledge of the nearshore bottom topography is of prime importance in many coastal engineering problems, ranging from beach morphology studies to design of coastal structures. Due to the active sediment transport, the bottom topography in shallow water is subjected to large changes on various time scales, and it is thus desirable to develop a method allowing for easy and continuous monitoring/prediction of topographical changes. The present study deals with a class of methods, referred to as *Depth Inversion Algorithms* (DIAs), in which these changes are predicted based on characteristics of shoaling waves measured on the ocean surface, e.g., using remote sensing techniques (e.g., Dugan *et al.*, 1996).

Ocean waves propagating toward a shore are usually the result of the superposition/interaction of multi-frequency and multi-directional wave components, whose distribution of energy can be represented by a directional wave spectrum. When such waves have been generated by far distant storms, however, they often reach the shore as long-crested swells, with a leading (spectral peak) frequency and

---

[1] In *Proc. of WAVES97 Intl. Conf.* (in press)

[2] Distinguished Associate Professor, Dpt. of Ocean Engng., University of Rhode Island, Narragansett, RI 02882. Tel.: (401) 874-6636; Fax.: (401) 792-6837; http://www.oce.uri.edu/~grilli

a main direction of propagation (generally oblique to the coast with some directional spreading) accounting for most of the energy contained in the wave field. In this case, waves are well represented by an equivalent (significant) periodic swell of deep water height H_o, period T, and direction θ_o with respect to the shore. Upon reaching mildly sloping shallow water areas, such swells shoal-up and refract as a function of the bottom depth variation, to end up breaking on the beach/shore and dissipating most of their energy; at this stage, due to refraction, the waves usually appear to be nearly parallel to the shore (i.e., $\theta \ll 1$). Coastal currents resulting from the combined effects of tides, winds, local estuaries, wave breaking, and meso-scale oceanic circulation, may also influence wave propagation during shoaling.

Although more complex cases will be addressed in future work, the present study will be limited to periodic waves propagating in a direction normal to the shore (i.e., $\theta_o = 0$). The coastal topography will be assumed to be nearly constant in the along-shore direction and mildly sloping in the cross-shore direction. Hence, the problem will be essentially a two-dimensional (2D) one in the vertical plane. It will also be assumed that there are no significant mean currents, except for those induced by waves in the cross-shore direction (mean mass transport, undertow).

Remote sensing techniques used in combination with DIAs measure the modulations of the slope of scatterers dispersed on the ocean surface (e.g., capillary waves), due to longer propagating gravity waves. Assuming a long-crested periodic swell, shoaling-up towards a long straight coast, with fairly straight and parallel bottom contours (i.e., the rather idealized 2D case introduced above), the swell's spatial phase variations can be retrieved from such measurements, in the direction x normal to the shore, using a relevant Modulation Transfer Function (MTF; Smith, 1997; Dugan, 1997b; Williams and Dugan, 1997). Phases, in turn, can be used to calculate variations of wavelength $L(x)$ and, when two "snapshots" of the ocean surface are taken over a short period of time Δt (ensuring a quasi-steady wave field; typically a few seconds over a a period of several tens of seconds for airborne remotely sensed data; Dugan, 1997a), phase celerity variations can also be obtained as, $c(x) \simeq \Delta x_p / \Delta t$ (where Δx_p denotes the distance between two successive locations of a line of constant phase in the snapshots). From the L and c data, wave period can be estimated as, $T \simeq L/c$. Using a wave theory in combination with this data, the bottom depth variation $h(x)$ can be obtained from an *inverted* dispersion relationship.

In most state-of-the-art DIAs, *linear wave theory* is still the basis for depth inversion (Dugan, 1997b; Williams and Dugan, 1997). This theory predicts wave celerity as a function of depth and period as (e.g., Dean and Dalrymple, 1984),

$$c_l = c_o \tanh kh \quad ; \text{with} \quad k = \frac{2\pi}{T\, c_l} \quad , \quad c_o = \frac{g\,T}{2\pi} \, , \tag{1}$$

the deep water wave celerity, and g the acceleration of gravity. No wave height effects are included in Eq. (1). These, according to Stokes theory, only become significant at third-order in kH, resulting in so-called *amplitude dispersion* effects which make higher waves travel faster. As we will see, significant errors in shallow water depth prediction (mostly an overprediction) can result from neglecting amplitude dispersion effects in DIAs. Moreover, the largest errors will be shown to occur in areas where depth is the most subject to change and thus depth information is the most needed. [This was recently pointed out by Dugan (1997b) and Williams and Dugan (1997), who used a DIA based on linear wave theory to analyze field data.] To account for amplitude dispersion effects and correct the wave celerity, simultaneous wave height data $H(x)$ is required. Such information can, in principle, be obtained using radar altimetry based on traveling times of radar waves. Accurate height measurements based on remote sensing techniques such as Synthetic Aperture Radar (SAR), however, are still quite problematic under the current state of the technology (Smith, 1997).

To illustrating the key features of depth-inversion in shallow water, it will first be assumed that a data set of simultaneous (c, L, H) values is available for a series of x locations in the cross-shore direction. As no existing theory can accurately provide celerity and height variations for large finite amplitude waves shoaling over arbitrary sloping bottom, results from computations of wave shoaling in a *fully nonlinear* numerical wave tank (NWT) will be used to develop semi-empirical relationships. A new DIA (referred to as DIA1) will be developed to process this data and predict the bottom depth variations. After validating and testing DIA1, an extension which eliminates the use of H and only relies on phase information (referred to as DIA2) will be proposed, together with the presentation of some preliminary results. More work about this however is needed.

Computation of wave shoaling in a NWT

Many past studies have attempted to predict wave shoaling transformations over an arbitrary bottom topography, using shallow water wave models derived from truncated series expansions of fully nonlinear potential flow (FNPF) equations, in terms of (supposedly) small parameters, such as $\delta = H/h$ and $\mu = kh$.

The standard Boussinesq equations (BE), for instance, are a weakly nonlinear and weakly dispersive approximation of depth-integrated FNPF equations, thus assuming, $\delta, \mu \ll 1$ and $\delta/\mu^2 = \mathcal{O}(1)$ (hence, $\mathcal{O}(\delta\mu^2, \mu^4)$ terms are neglected). Modified and/or extended BE models, in addition, have improved linear dispersion properties over a wider range of water depth (Madsen *et al.*, 1991; Nwogu, 1993). In the so-called fully nonlinear BE model by Wei *et al.* (1995), $\mathcal{O}(\delta\mu^2)$ terms are kept in the expansions and, hence, more strongly nonlinear waves can be accurately calculated than with standard BE models. Due to the truncations of the series, despite their satisfactory predictions for a wide range of water depth, BE models, even fully nonlinear, may still be insufficiently accurate to predict

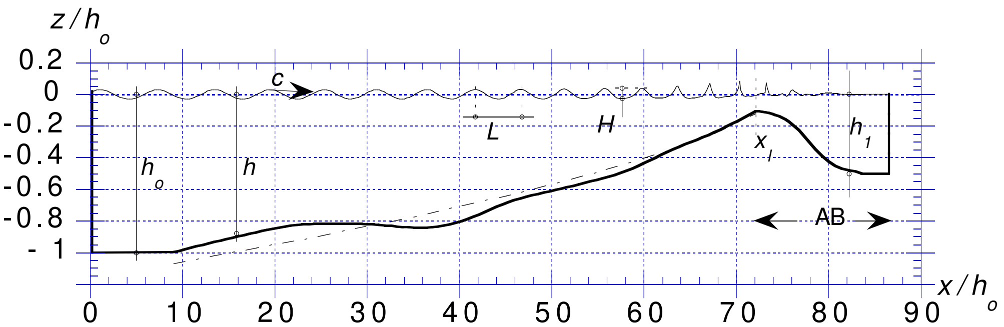

Figure 1: Typical sketch for periodic wave shoaling computations in the FNPF-NWT. The bottom topography (———-) corresponds to the average of five depth transects taken at Ft. Walton Beach (FL) on Sept. 29th, 1994 (Smith, 1997), with $h_o = 18.53$ m and an average slope 1:82; and (— - —) is the LSM fit to the topography : $h/h_o = 0.0758\,(74.20 - x/h_o)^{0.64}$ (with $R^2 = 0.98$).

wave shape and kinematics in very shallow water and close to breaking, where nonlinearity is strong and wave height is on the order of water depth.

Higher-order theories, such as the fully nonlinear steady wave theory (FSWT) by Sobey and Band (1991), have been introduced to account for strong wave nonlinearity. Such theories, however, assume wave periodicity and a stepwise bottom variation, and thus lack the key influence of wave skewness. As a result, they have been shown to provide an inaccurate prediction of shoaling wave characteristics in very shallow water, where waves take a forward skewed shape (Grilli and Horrillo, 1997b, 1998).

Recent advances in fully nonlinear models, directly based on FNPF equations without further approximation, i.e., so-called *numerical wave tanks* (NWT; see Tsai and Yue, 1996, for a review), have made it possible to calculate "numerically exact" properties of waves shoaling over arbitrary bottom topography, up to the breaking point, to within a few percent of laboratory measurements (Grilli, *et al.* 1994, 1997; Ohyama *et al.*, 1994; Grilli and Horrillo 1997ab, 1998). FNPF equations provide an accurate representation of surface waves, independently of depth or the value of parameters such as δ or μ. The only limitation is that friction and vorticity must be negligible, which is a rather good approximation before waves break (Dommermuth *et al.*, 1988). In FNPF-NWTs, mechanisms are provided for wave generation at an offshore boundary and wave energy absorption at the shore, before breaking occurs (Fig. 1). More details are given in the following.

Governing equations and boundary conditions

A typical domain for wave shoaling computations in the FNPF-NWT is sketched in Fig. 1. Waves are long-crested and propagate in the x direction normal to the shore. The NWT is defined by the free surface, the bottom, a leftward wavemaking boundary and a rightward absorbing boundary. Fully Nonlinear Potential Flow

(FNPF) equations are solved in the NWT, using a higher-order Boundary Element Method (BEM) based on Green's 2nd identity (Grilli *et al.*, 1989; Grilli and Subramanya, 1996). These equations are the governing continuity equation, a no-flow condition on the bottom, nonlinear kinematic and dynamic conditions on the free surface and specified velocity and accelerations on the leftward and rightward boundaries (see Grilli and Subramanya, 1996, and Grilli and Horrillo, 1997a, for details). Free surface equations are time integrated using second-order Taylor series expansions, expressed in terms of a time step and of the Lagrangian time derivative (Grilli *et al.*, 1989).

Although this NWT is general, incident waves in the present study are assumed to be periodic progressive waves. Following Grilli and Horrillo (1997a), in order to get permanent form finite amplitude incident waves, so-called zero-mass-flux *streamfunction waves* (SFW) are generated on the model leftward boundary. These waves, unlike finite amplitude waves produced by a wavemaker, do not exhibit the generation of higher-order harmonics and the beat phenomenon observed in wave tanks, as they propagate over constant depth. Since nonlinear waves have a non-zero mass flux, to ensure constant volume in the NWT, incident SFW's are generated together with a mean current, equal and opposite to their period-averaged mass transport velocity.

In a FNPF-NWT, computations can model overturning waves but, by nature, are limited to the time prior to that at which touch-down of a breaker jet first occurs. This does not pose problems when solitary waves are used in the analysis (Grilli *et al.* 1994, 1997). For periodic waves, however, an *absorbing beach* (AB) must be used to dissipate the energy of each successive incident wave, hence both eliminating reflection and preventing waves from breaking at the top of the slope, while letting them shoal up to very close to breaking. In the NWT, the AB is specified over a shallower region in the upper part of the slope, whose geometry is assumed somewhat similar to a natural bar on a beach (Fig. 1). Energy absorption combines both free surface and lateral absorption, with an adaptive calibration of the absorption coefficient (Grilli and Horrillo, 1997a). Grilli and Horrillo (1997b, 1998) showed that, using these methods, reflection from the AB could be reduced to a few percent. Reflection from the sloping bottom, however, still occurs as it does in nature, but it is rather small for mild slopes.

Computation of shoaling wave properties

In computations of periodic wave shoaling, the NWT is assumed to be initially at rest (cold start). At the start of computations, incident periodic waves are generated in the NWT by specifying their shape and kinematics along the leftward *wavemaking* boundary. An initial tapering function is used over the first three periods. For zero-mass-flux SFWs, wave kinematics is obtained as a function of initial wave height H_o, period T, and initial depth h_o (Grilli and Horrillo, 1997a). As waves initially behave nearly linearly up to a relative depth $k_o h \simeq$

No.	H_o'	T'	$H_o^{'*}$	k_o'	$k_o h_o^*$	$k_o H_o$	c_o'
1	0.0435	5.5	0.04	1.305	0.79	0.0568	0.8754
2	0.0653	5.5	0.06	1.305	0.79	0.0852	0.8754
3	0.0871	5.5	0.08	1.305	0.79	0.1137	0.8754
4	0.0424	6.5	0.04	0.934	0.56	0.0396	1.0345
5	0.0636	6.5	0.06	0.934	0.56	0.0594	1.0345
6	0.0848	6.5	0.08	0.934	0.56	0.0792	1.0345
7	0.0409	7.5	0.04	0.702	0.42	0.0287	1.1937
8	0.0614	7.5	0.06	0.702	0.42	0.0430	1.1937
9	0.0819	7.5	0.08	0.702	0.42	0.0575	1.1937

Table 1: Input characteristics of incident waves in the NWT : H_o' deep water wave height; T' wave period; $H_o^{'*}$ wave height at initial offshore depth $h_o^{'*} = 0.6$, in the NWT; $k_o' = (2\pi/T')^2$ and $c_o' = T'/2\pi$ (linear) deep water wave number and celerity, respectively. Primes denote dimensionless variables, where distances have been divided by h_o, a reference depth, and times by $\sqrt{h_o/g}$.

$0.4 - 0.5$, computations are started in intermediate water, in depth h_o^*, and deep water characteristics are back calculated using linear wave theory. Table 1 gives a summary of wave parameters for the computations used for calibrating the DIAs. Table 2 gives the same parameters for the DIAs' validation applications.

In each case, envelopes of crest and trough elevations are calculated for successive waves, and wave height $H(x)$ is thus obtained. Using the same results, the phase velocity of successive waves is calculated as $c(x) = dx_c/dt$, where $x_c(t)$ denotes the instantaneous crest location of a given wave; the spatial wave length, which will be used in the DIAs (see next section), is calculated two ways : (i) as the horizontal distance between a crest and the previous one, $L_c(x)$; or (ii) between a trough and the next one, $L_t(x)$. After the initial transient wave front has been absorbed in the AB, results show that values of H, c, and L are well reproduced for successive incident waves in the NWT. To eliminate the small remaining differences between successive waves, wave properties are averaged over 4 to 6 waves.

For periodic waves shoaling over mild slopes, Grilli and Horrillo (1997b, 1998) used this FNPF-NWT to calculate celerity and height variations for many different incident waves shoaling over mildly sloping bottoms. They showed that, although a slope is needed in the tank to induce the necessary skewness in shoaling waves, for a range of mild slopes between 1:35 and 1:70, c and H (and most other results) do not depend very much on the magnitude of the slope, provided results are compared for the same normalized depth $k_o h$ or kh. Full nonlinearity, however, is important in shallow water and large differences (up to 80%) may

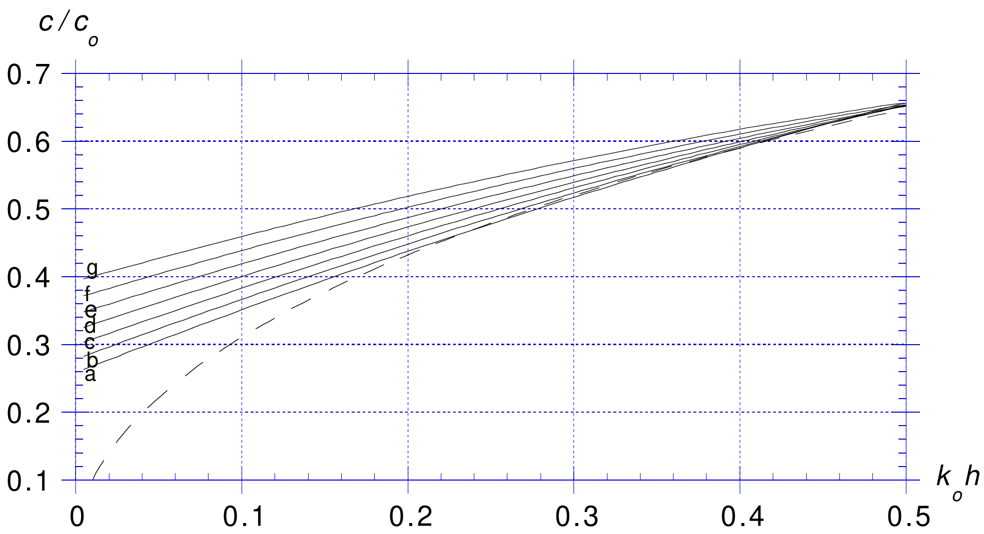

Figure 2: Empirical fit of wave celerities c/c_o computed in NWT for $s = 1 : 50$, based on Eq. (2). Curves a to g correspond to $k_oH_o = 0.02$ to 0.14 by step 0.02. (– – –) $c_l/c_o = \tanh kh$, linear wave celerity.

occur between predictions of linear or weakly nonlinear wave theories, and the fully nonlinear results. In the present study, detailed results computed by Grilli and Horrillo (1997b) for nine cases of periodic waves shoaling over a 1:50 plane slope (Table 1) are used to develop and calibrate the two new DIAs, by which a monotonously decreasing bottom topography can be accurately predicted based on waves properties, such as $c(x)$, $L(x)$, $H(x)$, and wave spatial asymmetry, measured on the free surface. According to Grilli and Horrillo's results, the DIAs should be applicable to slopes 1:35 and milder. The new DIAs will be validated by predicting the bottom topography, using wave shoaling characteristics computed in the NWT, for more complex cases than in the original calibration computations (Table 2).

In the results, when not otherwise mentioned, primed variables indicate non-dimensional variables in which lengths have been divided by h_o, a reference depth, and times by $\sqrt{h_o/g}$.

Depth Inversion Algorithms

Celerity and height variations for periodic waves

Results of computations in the FNPF-NWT, for periodic waves shoaling over a 1:50 slope, with parameters listed in Table 1, have been analyzed in detail by Grilli and Horrillo (1997b, 1998). Over mild slopes, two important parameters were shown to govern wave celerity and height variations, k_oH_o and k_oh, which respectively express deep water wave steepness and relative depth.

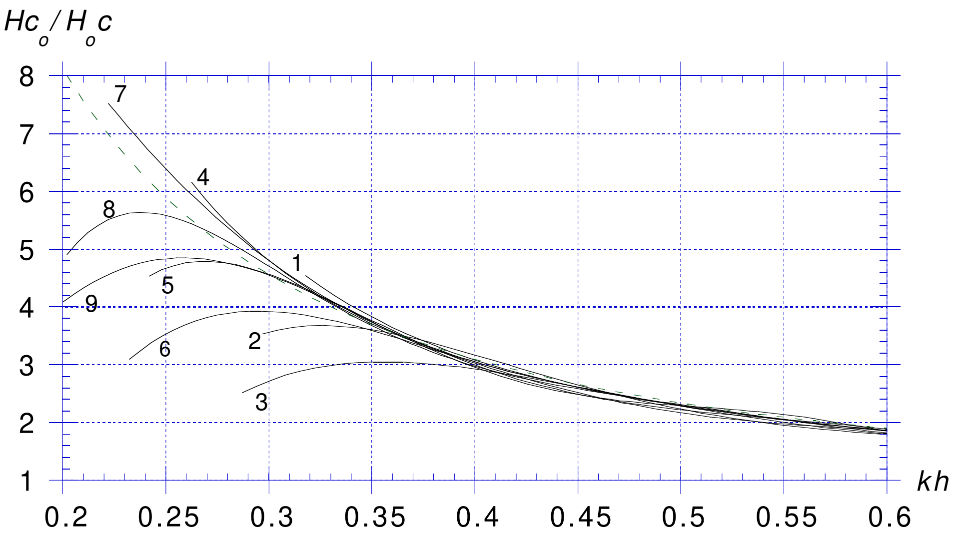

Figure 3: Normalized wave steepness $kH/k_oH_o = Hc_o/H_oc$ computed in the NWT for the 9 cases listed in Table 1. (- - - -) $g_l(kh)$ for linear theory.

To express wave celerity for other values of the two parameters than for the cases in Table 1, and considering the low sensitivity of results to detailed bottom shape for mild slope, an empirical function is LSM fitted to the computed celerities, in the depth region where discrepancies with linear wave theory are significant, i.e., for $k_oh \leq 0.5$. A bi-quadratic function of the two parameters is found to give good results,

$$\begin{aligned} \frac{c}{c_o} &= A_0 + A_1\,(k_oh) + A_2\,(k_oH_o) + A_3\,(k_oh)\,(k_oH_o) \\ &+ A_4\,(k_oh)^2 + A_5(k_oH_o)^2 \end{aligned} \tag{2}$$

with A_i = (0.2397,1.0063,0.9118,-2.2405,-0.3299,1.3292) and $R^2 = 99.8\%$. Fig. 2 shows c/c_o variations calculated based on Eq. (2), for $k_oh = 0$ to 0.5 and $k_oH_o = 0.02$ to 0.14 by steps of 0.02. In Fig. 2, the nonlinear celerity curve a ($k_oH_o = 0.02$, i.e., for the smaller incident steepness) agrees well with linear wave theory, down to depth $k_oh = 0.2$. For smaller steepness, an interpolation between these curves can be made.

Grilli and Horrillo (1997b, 1998) showed that, computed wave height H is well predicted by, $H_o(c/c_o)\,g_l$, in which $g_l = k_lH_l/k_oH_o$ is the normalized wave steepness predicted by linear wave theory,

$$g_l = (\tanh kh)^{-3/2}\,[1 + \frac{2kh}{\sinh 2kh}]^{-1/2} \tag{3}$$

and c/c_o is the nonlinear celerity. When applied to the results of the cases in Table 1, Eq. (3) explains at least 98% of the variance of the monotonous part of the numerical results for $H/(H_o\,c/c_o)$ (Fig. 3). Eq. (3) can thus be used in the DIA's, to estimate H_o, when a set of simultaneous values of H and c is available.

Depth Inversion Algorithm for (c, H, L) data (DIA1)

In this depth inversion problem, referred to as DIA1, $c(x)$, $H(x)$ and ($L_c(x)$,$L_t(x)$) are assumed to be known from simultaneous free surface observations, at locations x_i, for $i = 1, ..., N$. The problem thus consists in predicting $h(x_i)$, for $i = 1, ..., N$, based on these observations. Assuming, Eq. (2) represents the true nonlinear celerity variation, independent of the details of bottom topography for mildly and monotonously sloping bottom, we can invert Eq. (2) to predict the depth corresponding to a known celerity. Since, for nonlinear waves, celerity varies with k_oH_o, particularly in shallow water, both T and H_o must also be retrieved from the data. For periodic waves in stationary propagation, $T = L/c$, where L is the "true" wavelength. After several numerical tests, it was found that T was accurately predicted using the average of L_c and L_t, as the mean of, $[(L_c(x) + L_t(x))/(2\,c(x))]$, over the x_i locations ($i = 1, ..., N$). As explained above, the deep water wave height is found by calculating the mean of, $[H(x)/(g_l\,(c(x)/c_o))]$, over the x_i locations ($i = 1, ..., N$). Since g_l is only known as a function of $kh = k_oh(x)/(c(x)/c_o)$, H_o is iteratively predicted, by using Eq. (3) together with the inverted Eq. (2) which predict k_oh as a function of k_oH_o and c/c_o.

In DIA1, after predicting T, a first guess is made for H_o, as the wave height observed at the most offshore location. A first depth variation $h(x_i)$ is calculated for this guess using the inverted Eq. (2) and the values of c observed at points $x_i; i = 1, ..., N$. Based on this, a new corrected value of H_o is calculated from H and c values, as explained above. The procedure is repeated until convergence is reached on H_o. Note, for known c/c_o and k_oH_o, Eq. (2) is easily inverted as a quadratic equation for k_oh.

Depth Inversion Algorithm for $(c, H, s_2/s_1)$ data (DIA2)

An extension of DIA1, referred to as DIA2, which eliminates the use of H and only relies on phase information is proposed in the following.

When initially left-right symmetrical waves shoal-up a sloping bottom, due to nonlinearity, they become increasingly asymmetric (i.e., skewed). In actual depth inversion problems, long time series of wave elevation from which skewness could be calculated are not available whereas spatial variations are (i.e., the "snapshots"). Wave asymmetry can be spatially quantified by the ratio of forward to backward wave slopes, $s_2(x) = H_2/L_2$ and, $s_1(x) = H_1/L_1$, respectively, in which (L_1, L_2) and (H_1, H_2) denote horizontal and vertical distances from a crest to the previous and next troughs, respectively. Since wave height does not change too much over one wavelength, the approximate slope ratio, $s_2/s_1 \simeq L_1/L_2$, can be used as a measure of wave left to right spatial asymmetry. Grilli and Horrillo (1997b, 1998) calculated the variation of this parameter for the 9 cases in Table 1 and showed that it has a high degree of correlation with wave skewness.

As a substitute to the wave height data used in DIA1 to retrieve H_o, values of

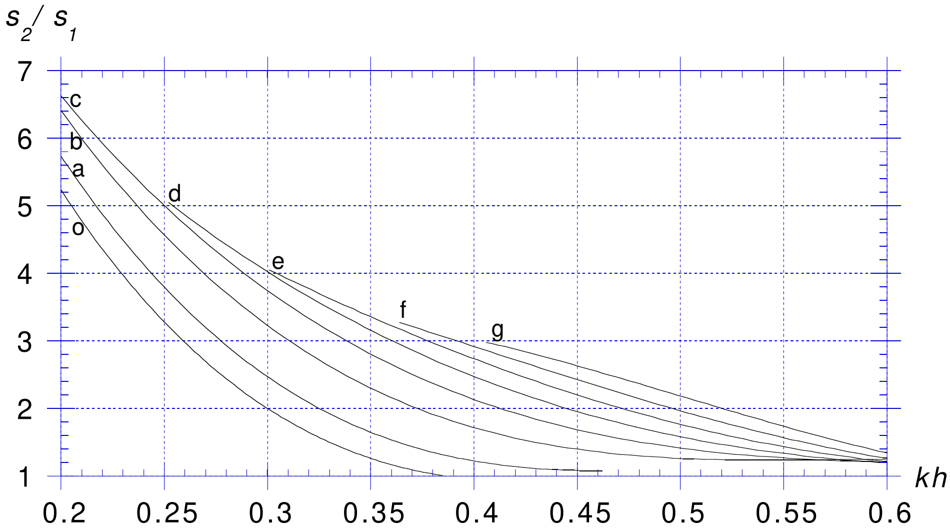

Figure 4: Empirical fit of wave left-right asymmetry s_2/s_1 computed in NWT for $s = 1:50$ (Table 1), based on Eq. (4). Curves a to g correspond to $k_oH_o = 0.02$ to 0.14 by step 0.02, as in Fig. 4, and curve o to $k_oH_o = 0.01$. Note, curves have been limited based on $s_2/s_1 \geq 1$ and on the estimation of breaking locations for the steeper waves.

s_2/s_1 calculated from measured phase information can be used to estimate k_oH_o. To do so, an empirical function of kh and k_oH_o is LSM fitted to the data for the cases in Table 1,

$$\begin{aligned}
\frac{s_2}{s_1} &= \{\, B_0 + B_1\,(kh) + B_2\,(kh)^2 + B_3\,(kh)^3 \,\} \\
&+ \{\, B_4 + B_5\,(kh) + B_6\,(kh)^2 + B_7\,(kh)^3 \,\}\,(k_oH_o) \\
&+ \{\, B_8 + B_9\,(kh) + B_{10}\,(kh)^2 + B_{11}\,(kh)^3 \,\}\,(k_oH_o)^2 \qquad (4)
\end{aligned}$$

with $B_i =$ (22.329, -138.01, 284.70, -187.90, -3.7352, 80.763, -2708.3, 2260.0, -1228.8, 3561.2, -670.52, -2907.8) and $R^2 = 96.6\%$. Fig. 4 shows s_2/s_1 variations calculated based on Eq. (4) for $kh = 0$ to 0.6 and $k_oH_o = 0.02$ to 0.14 by steps of 0.02. For given values of s_2/s_1 and kh, Eq. (4) is a quadratic equation for k_oH_o.

Hence, in DIA2, after predicting T as in DIA1, a first guess is made for H_o, as a small but finite value. A first depth variation $h(x_i)$ is calculated for this guess, using the inverted Eq. (2) and the values of c observed at points x_i ($i = 1, ..., N$), as in DIA1. Based on this, $kh = k_oh(x)/(c(x)/c_o)$ is obtained and a new corrected value of H_o is calculated from s_2/s_1 values using Eq. (4). The procedure is repeated until convergence is reached on H_o.

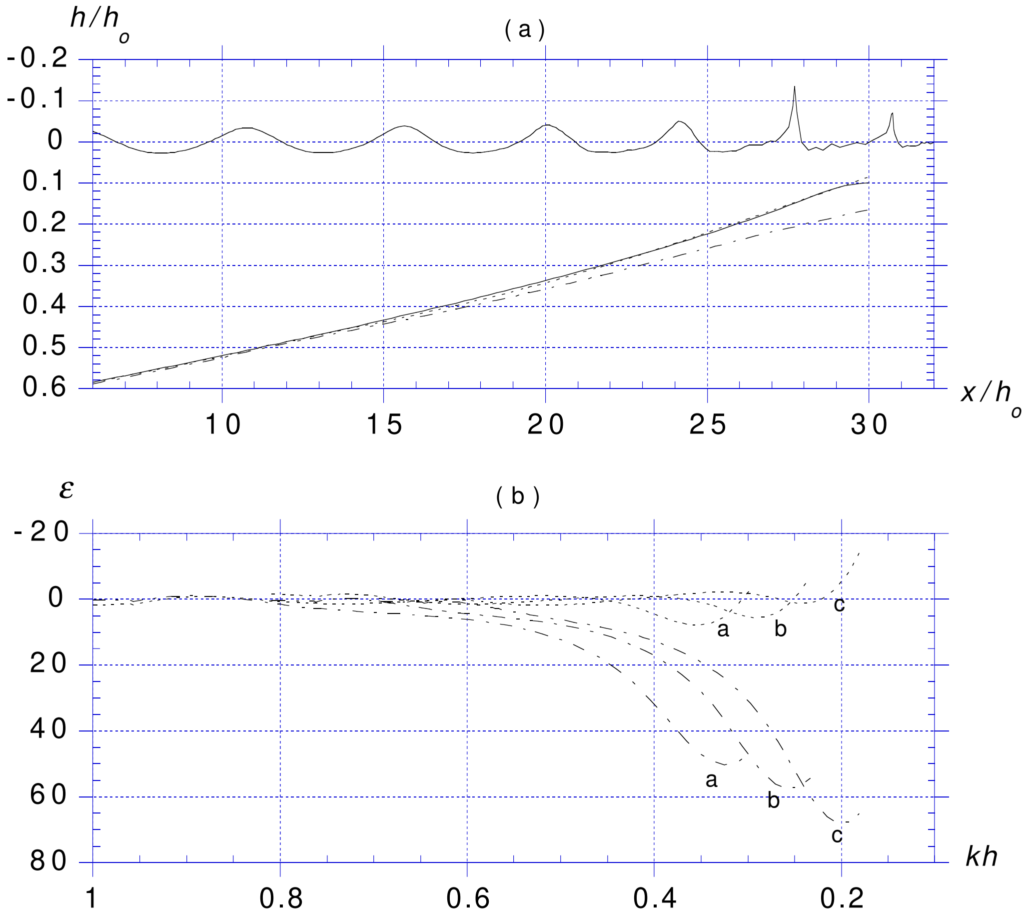

Figure 5: Depth inversion for an equilibrium beach with average slope 1:50. (a) Case n3 (Table 2) : (——) $\eta(x)$ at $t' = 106.9 = 14.3T'$; (———) True bottom topography $h(x)$; (- - - - - -) estimated topography with DIA1 [Note, $h(x)$ estimates are found closely similar with DIA2]; (— - —) estimated topography with linear dispersion relation. Note, the bottom is plotted up to the entrance of the AB in the NWT (Fig. 1). (b) Relative errors of depth prediction, $\varepsilon = (h_i - h(x_i))/h_i$, for cases a: n1 , b: n2, c: n3, with : (- - - - - -) DIA1; (— - —) linear dispersion relation.

Case	T'	T'_p	H'_{po}	rms_h	ε_{hm}	rms_l	ε_{lm}	rms_c	rms_H
n1	5.5	5.52	0.0646	2.1	8.0	14.6	50.3	0.6	2.7
n2	6.5	6.52	0.0625	1.7	7.1	17.0	57.6	0.5	2.0
n3	7.5	7.51	0.0602	2.0	13.9	20.5	67.9	0.4	2.0

Table 2: Results for three depth inversion cases with DIA1 on a natural beach : T'_p predicted wave period; H'_{po} predicted deep water wave height; (rms_h, ε_{hm}), root mean square and maximum relative errors (%) for depth prediction with DIA1; (rms_l, ε_{lm}), root mean square and maximum relative errors (%) for depth prediction with the linear dispersion relation; (rms_c, rms_H) root mean square errors for direct celerity and depth predictions.

Numerical validation of depth inversion algorithms

Depth Inversion Algorithm for (c, H, L) data (DIA1)

DIA1 was validated for a bottom topography following Dean's equilibrium beach profile (Dean, 1991), i.e., a *natural beach* with an average slope 1:50. Direct computations were made in the FNPF-NWT, for the shoaling of incident SFWs, with height H^*_o and period T at depth $h^*_o = 0.6h_o$, and a numerical data set of about 100 simultaneous (x, c, H, L_c, L_t) values per case was numerically generated. DIA1 was applied to this data set and a prediction of the bottom topography $h(x)$ made. This prediction was compared to the actual topography, thus assessing the accuracy of DIA1, in terms of rms-errors or model skill. The accuracy of wave period, height, and celerity predictions was also evaluated.

According to Dean's theory, natural beaches tend to follow an average bottom depth variation defined as, $h = A(x^* - x)^{2/3}$, with x^* denoting a constant, function of the location of the toe of the slope in depth h^*_o, and A, a constant depending on the specified average slope (which actually is related to the mean sediment grain size). In Fig. 1, for instance, the measured bottom topography at Ft. Walton Beach, FL (Smith, 1997) was sketched as an example of a natural beach, and an average equilibrium shape was fitted as $h/h_o = 0.0758\,(74.20 - x/h_o)^{0.64}$; hence, $0.64 \simeq 2/3$. The curve fit had an $R^2 = 0.98$ which indicates a good overall agreement. The equilibrium beach profile has a milder slope in deeper water and a steeper slope in shallower water, than the average value (1:82 in the case of Fig. 1). In the present case, for a natural beach with 1:50 average slope starting in depth $h'^*_o = 0.6$, the slope in the NWT varies between 1:65 and 1:32, up to the AB (in depth $h' = 0.1$). Hence, it covers the range of slopes over which DIA1 was calibrated.

To validate DIA1, three shoaling cases, referred to as n1, n2, and, n3 in Table 2, were computed in the FNPF-NWT, for the selected natural beach, using three different incident waves of height $H_o^{'*} = 0.06$ and periods $T' = 5.5$, 6.5, and 7.5, respectively, resulting in waves of decreasing incident steepness. These cases, in fact have the same incident wave data as cases 2, 5, and 8 in Table 1, which can be consulted for the values of some parameters. Figure 5a shows both a shoaling wave profile and results of the application of both DIA1 and the linear dispersion relation to the depth inversion for case n3. Table 2 gives general data and results for the three cases, and Figure 5b shows depth prediction errors for the three cases, using DIA1 or the linear dispersion relation.

Predicted wave periods T_p' were found to be within 0.4, 0.3, and 0.1% of the true period, and deep water wave heights H_{po}' within 1.1, 1.7, and 1.9% of the true height, for cases n1, n2 and n3, respectively (Table 2). For the direct prediction of c, DIA1 has very small rms_c errors of 0.6, 0.7, and 0.4% for cases n1, n2 and n3, respectively (Table 2). All the $k_o H_o$ values for these cases are in the range of the original computations based on which Eq. (2) was derived, but the bottom topography, however, is different. The low rms_c values, hence, further confirm the hypothesis at the basis of our DIAs that celerity can be predicted for a variety of mildly sloping topographies based on results obtained for a simple plane slope. For the final prediction of H, after iterations based on Eq. (3), the algorithm gives rms_H errors of 2.7, 2.0 and 2.0% for cases n1, n2 and n3, respectively (Table 2). In Fig. 5b, it is clear that DIA1 provides a much more accurate prediction of the bottom topography than when using the linear dispersion relation. Depth prediction errors for DIA1 are only a few percent for most of the wave propagation distance (rms_h errors are 2.1, 1.7 and 2.0%, respectively, in Table 2), whereas errors with the linear dispersion are always larger and reach very large values (order 50-70%), particularly, in the shallower water region for $kh < 0.60$.

Depth Inversion Algorithm for $(c, H, s_2/s_1)$ data (DIA2)

Depth inversion was repeated using DIA2, for the three cases of Table 2, based on the same data but using the calculated values of s_2/s_1 instead of H.

Small rms_h errors of 2.1, 3.4, and 3.2 %, respectively, were obtained for the depth prediction, using the LSM fit of Eq. (4) to the data from the 9 cases in Table 1 to estimate H_o. Errors on the direct prediction of $H(x)$, however, were larger than with DIA1 (rms_H =2.7, 13.4, and 13.1 %, respectively), indicating that detailed information on wave height is not so important, provided H_o is correctly estimated. These good results confirmed that DIA2 is also a viable depth inversion method.

Conclusions

Two DIAs were developed based on empirical representations of results of computations in a FNPF-NWT, for periodic wave shoaling on mild slopes. The DIAs were applied to depth inversion, for a natural beach profile, using numerically calculated series of spatial data for $(c, L_c, L_t, H, s_2/s_1)$. In all cases, rms-errors for the depth predictions were found to be less than a few percent (1.7-2.1% for DIA1; 2.1-3.2% for DIA2), whereas depth predictions based on the linear dispersion relation gave rms-errors 5 to 10 times larger (14.6-20.5%). Whereas rms-errors were slightly larger with DIA2 than with DIA1, they are still significantly smaller than those corresponding to linear wave theory (3 to 7 times smaller).

Although more work is needed, these preliminary results clearly indicate the relevance of DIA1 and DIA2's approach for carrying out depth inversion. Since DIA2 is purely based on parameters derived from wave phase information, it has a potential applicability to field data. Results also indicate that state-of-the-art depth inversion methods based on the linear dispersion relation may lead to large errors (50-70%) for the depth prediction in very shallow water, where wave nonlinearity is large and amplitude dispersion effects cannot be neglected in the celerity relationship.

Finally, it should also be pointed out that the same bottom topography used in cases n1, n2, and n3 was predicted by DIA1 and DIA2, with the same level of accuracy (i.e., rms error), for the three different incident waves. Hence, this indicates that, in actual field situations, results obtained for several incident waves with different characteristics could be averaged to obtain a better prediction of the depth variation.

Future work will address both non-periodic waves and non-monotonous topographies (i.e., barred beaches).

Acknowledgements

This publication is the result of research sponsored by the US Naval Research Laboratory, Stennis Space Center, grants N-00014-95-1-G607 and N-00014-96-C012, from the Remote Sensing Division (code 7240). The kind assistance of Dr. Peter Smith from NRL-SSC and Dr. John Dugan from Areté Associates is gratefully acknowledged.

References

Dean, R.G., Equilibrium Beach Profiles : Characteristics and Applications *J. Coastal Res.,* **7** (1), 53-84, 1991.

Dean, R.G. and Dalrymple R.A., *Water Wave Mechanics for Engineers and Scientists* Prentice-Hall, 1984.

Dommermuth, D.G., Yue, D.K.P., Lin, W.M., Rapp, R.J., Chan, E.S. and Melville, W.K., Deep-Water Plunging Breakers : a Comparison between Potential Theory and Experiments *J. Fluid Mech.* **189,** 423-442, 1988.

Dugan, J. Personal communication, 1997a.

Dugan, J. Bathymetry measurements from long range airborne imaging systems. In *Proc. 4th Intl Conf on Remote Sensing for Marine and Coastal Environments*, Orlando, FL, 1997b.

Dugan, J., Forsyth, C., Suzukawa. H. and Farber, M. Ocean wave dispersion surface measured with airborne IR imaging system. *IEEE Trans. Geosci. and Remote Sensing*, **34**(4), 182-1284, 1996.

Grilli, S.T. and Horrillo, J. Numerical Generation and Absorption of Fully Nonlinear Periodic Waves. *J. Engineering Mech.,* **123** (10), 1060-1069, 1997a.

Grilli, S.T. and Horrillo, J. Fully Nonlinear Properties of Periodic Waves Shoaling over Slopes. In *Proc. 25th Intl. Conf. on Coastal Engineering* (ICCE25, Orlando, USA, September 96), Vol. **1**, pps. 717-730. ASCE edition, 1997b.

Grilli, S.T. and Horrillo, J. Computation of Properties of Periodic Waves Shoaling over Mild Slopes in a Fully Nonlinear Numerical Wave Tank. *J. Geophys. Res.* (submitted), 1998.

Grilli, S., Skourup, J., and Svendsen, I.A., An Efficient Boundary Element Method for Nonlinear Water Waves, *Engng. Analysis with Boundary Elements,* **6**(2), 97-107, 1989.

Grilli, S.T. and Subramanya, R., Numerical Modeling of Wave Breaking Induced by Fixed or Moving Boundaries. *Computational Mech.,* **17,** 374-391, 1996.

Grilli, S., Subramanya, R., Svendsen, I.A. and Veeramony, J. Shoaling of Solitary Waves on Plane Beaches. *J. Waterway Port Coastal and Ocean Engng.,* **120** (6), 609-628, 1994.

Grilli, S., Svendsen, I.A. and Subramanya, R., Breaking Criterion and Characteristics for Solitary Waves on Slopes. *J. Waterway Port Coastal and Ocean Engng.,* **123** (3), 102-112, 1997.

Madsen, P.A., Murray, R. and Sorensen, O.R., A New Form of the Boussinesq Equations for Nearshore Wave Propagation. *Coastal Engng.,* **15,** 371-388, 1991.

Nwogu, O., An Alternative Form of the Boussinesq Equations for Nearshore Wave Propagation, *J. Waterway, Port, Coast. Ocean Engng*, **119**(6), 618-638, 1993.

Ohyama, T., Beji, S., Nadaoka, K., and Battjes, J.A., Experimental Verification of Numerical Model for Nonlinear Wave Evolution. *J. Waterway Port Coastal and Ocean Engng.,* **120**(6), 637-644, 1994.

Smith, P. Personal communication, 1997.

Sobey, R.J. and Bando, K., Variations on Higher-order Shoaling. *J. Waterway Port Coastal and Ocean Engng.,* **117** (4), 348-368, 1991.

Tsai, W.T. and Yue, D.K.P., Computation of Nonlinear Free-surface Flows, *Annu. Rev. Fluid Mech.,* **28,** 249-278, 1996.

Wei, J., Kirby, J.T, Grilli, S.T. and R., Subramanya, A Fully Nonlinear Boussinesq Model for Surface Waves. I. Highly Nonlinear Unsteady Waves. *J. Fluid Mech.,* **294,** 71-92, 1995.

Williams, J.Z. and Dugan, J. Bathymetry measurements using electro-optical remote sensing. In *4th Intl Conf on Remote Sensing for Marine and Coastal Environments*, Orlando, FL, 1997